ACS APPLIED MATERIALS & INTERFACES

RESEARCH ARTICLE

www.acsami.org

A Reproducible SERS Substrate Based on Electrostatically Assisted APTES-Functionalized Surface-Assembly of Gold Nanostars

Qianqian Su, Xiaoyuan Ma, Jian Dong, Caiyun Jiang, and Weiping Qian*

State Key Laboratory of Bioelectronics, School of Biological Science and Medical Engineering, Southeast University, Nanjing 210096, P. R. China

Supporting Information

ABSTRACT: A SERS active gold nanostar layer on the surface of ITO glass slip has been prepared by a low-cost electrostatically assisted APTES-functionalized surface-assembly method for SERS analysis. The two-dimensional morphology of the SERS substrate was examined by scanning electron microscopy. Comparative analysis revealed that the optical characteristics and SERS efficiency of these substrates varied as a function of nanostar morphology. It was found that the substrate assembled with the longest branches of nanostars generated the best SERS efficiency, whether the excitation source is 785 or 633 nm. The potential use of these substrates in detection applications was also investigated by using Nile blue A and Rhodamine 6G. The detection limits are 5×10^{-11} M and 1×10^{-9} M, respectively, when using the 785 nm excitation source. Apart from this high enhancement effect, the substrate here also shows extremely good reproducibility at the same time. All of these indicate that gold nanostars are a very good structure for SERS substrate assembly.

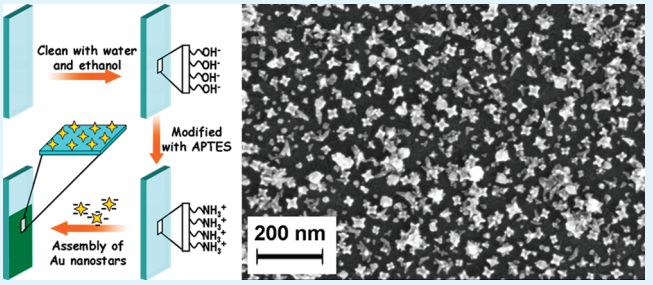

KEYWORDS: SERS, gold nanostar, reproducible substrate, electrostatically assisted APTES-functionalized surface-assembly, low-cost

INTRODUCTION

Surface-enhanced Raman scattering (SERS) spectroscopy has received a great deal of attention for its utility as a sensitive technique for chemical and biomedical analysis.[1−4] Theoretically, the enhancement effects have been attributed to two models, "chemical mechanism (CM)" and "electromagnetic mechanism (EM)".[5] The EM enhancement results from an increased field at the metallic nanoparticle surface which is a consequence of the interaction of the incoming laser radiation with electrons in the metal surface or collective oscillations of the metal electrons.[6] Because localized surface plasmon resonance (LSPR) has been considered to be the major contribution to the EM enhancement,[7] the engineering and fabrication of metal colloids with the ability of sustaining strong LSPR effect constitutes a hot research field in both nanoscience and SERS studies.[7−10]

However, whether SERS can achieve a broader application really depends on the SERS activity and the reproducibility of the SERS active substrates.[11] An ideal SERS substrate should be uniform, reproducible, and clean while exhibit high SERS activity. The electrostatically assisted APTES-functionalized surface-assembly method is a very facile way to obtain uniform, reproducible SERS substrate, but the main limit is that the obtained substrates usually do not have strong enough SERS enhancement. Gold nanostars, as one of the anisotropic structures, have been recently reported to yield extraordinary field enhancements for SERS,[12] especially at the tip of their branches. It has been reported that gold nanostars show stronger SERS enhancement than nanorods and nanospheres under similar experimental conditions.[6] Thus, the combination of these two aspects may provide a solution to the fabrication of a low-cost, large-scale, and reproducible SERS active substrate. The nanostar arrays reported by Rodríguez-Lorenzo et al.[13] could generate a $\sim 1 \times 10^{10}$ enhancement factor when using 1,5-naphtalenedithiol as analyte, but considering that the nanostar array was assembled on a gold substrate, it is may not be cost-efficient; Single nanostar on ITO surfaces with high enhancement effect (total enhancement $\sim 1 \times 10^{7}$) were made by Hrelescu et al.,[14] multilayer films were also mentioned in the report but little information on reproducibility or scalability was provided.

This paper reports the assembly of gold nanostars as reproducible SERS substrates via electrostatically assisted APTES-functionalized surface-assembly method and studies the SERS activities. We detailed the modification of the protocol reported by Xie et al.[15] and synthesized gold nanostars with controllable branch lengths. Then, these nanostars were immobilized on ITO surfaces by using electrostatically assisted APTES-functionalized surface-assembly as SERS active substrates. A comparison of these substrates' optical characteristics and SERS efficiency as a function of branch length was made, and the potential use of

Received: January 17, 2011
Accepted: April 29, 2011
Published: April 29, 2011

these substrates in detection applications were also investigated. There are two main advantages of our substrates: first, the fabricating progress of this substrate is simple, low-cost, reproducible, and equipment-independent, thus it is possible for large-scale production, even for commercial manufacture; second, the obtained substrates have extremely good uniformity, which is preponderant in quantitative analysis.

EXPERIMENTAL SECTION

Chemicals and Reagents. Ultrapure water from Milli-Q (Millipore, America, resistivity >18M) source was used throughout the experiments. 3-Aminopropyltriethoxysilane (APTES, 97%), from Sigma, was stored at 4 °C. Chloroauric acid terahydrate ($HAuCl_4 \cdot 4H_2O$), hydrochloric acid (HCl), nitric acid (HNO_3), and ethanol (C_2H_5OH) were all purchased from Nanjing Sunshine Biotechnology Ltd., China. Nile blue A (NBA) was purchased from Alfa Aesar. N-2-Hydroxyethylpiperazine-N′-2-ethanesulfonic acid (HEPES) was purchased from Shanghai Sangon Biological Engineering Technology & Services Co., Ltd., China. Rhodamine 6G (R6G) was purchased from Sigma. All reagents were used as received without further purification.

Synthesis of Gold Nanostars. Gold nanostars were synthesized by the protocol presented by Xie et al.[15] Briefly, aqueous stock solution of HEPES with concentration of 100 mM was prepared with ultrapure water, and pH was adjusted to 7.5 ± 0.5 at 25 °C by adding 1 M NaOH solution. Two milliliters of 100 mM HEPES (pH 7.5) was mixed with 3 mL of deionized water, followed by the addition of 24.25 mM $HAuCl_4$ solution volumes ranging from 40 to 115 μL, which yielded star branch lengths of 20 down to 0 nm, respectively. Without shaking, the color of each solution changed from light yellow to colorless and finally to purple/blue for smaller stars, to green for large stars, within 20 min.

UV−vis−NIR extinction spectra of gold nanostar samples were measured using a Shimadzu UV3150 UV−vis−NIR spectrophotometer. A JEM2100EX transmission electron microscopy (TEM) was used to image the morphology of gold nanostars at different conditions. TEM samples were prepared by drying a drop of the respective solution of the particles on carbon-coated copper grids.

Preparation of SERS-Active Substrates. The fabrication of APTES-functionalized ITO glass was carried out according to the literature procedures by our previous paper[16] and the literature reported by Enders et al.[17] All ITO glass slips were washed with Aqua Regia (HCl: HNO_3 in a 3:1 ratio by volume) and rinsed with ultrapure water for at least five times. The slips were further cleaned in ethanol with sonication for three times and dried at 70 °C for 2 h in an air oven. The cleaned ITO glass slips were vertically immersed in a 1% (v/v) ethanol solution of APTES in anhydrous ethanol at 70 °C for 2 h, rinsed three times in ethanol with sonication to remove silane excess, and dried for 2 h at 100 °C in an air oven.

Then, the silanized ITO glass slips were vertically dipped overnight into the stirred colloidal suspension of gold nanostars for the purpose of preparing Au nanostar layers. Also, blank ITO glass slips (that were not functionalized) were vertically dipped overnight into the stirred colloidal suspension of gold nanostars for the purpose of preparing control groups. Finally, these substrates were all washed with ultrapure water for three times and were dried for 30 min at 30 °C. Suitable substrates for SERS measurements were thus synthesized. A Zeiss ULTRA-plus scanning electron microscope (SEM) was used to image the morphology of Au nanostar layers at 15 kV.

SERS Measurements. For subsequent SERS experiments, two analytes were used, including NBA and R6G. The active substrates previously described were first vertically immersed in each analyte aqueous solution for 4 h at 4 °C and then left to dry at room temperature after rinsing several times with ultrapure water for SERS measurements.

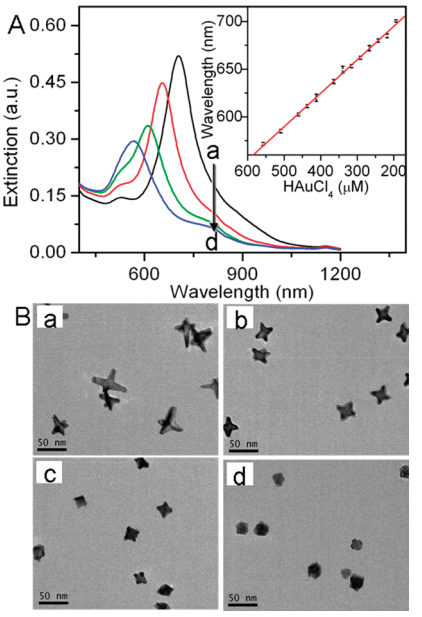

Figure 1. (A) UV−vis−NIR spectra of gold nanostars formed by reducing different concentrations of $HAuCl_4$ ((a) 194, (b) 315.3, (c) 436.5, and (d) 557.8 μM) solutions with 0.04 M HEPES solution. The calibration curve corresponding to the longitudinal plasmon resonance wavelength of the resulting gold nanostars at different concentrations of $HAuCl_4$ (from 194 to 557.8 μM) is shown as the insert. (B) TEM images of star samples corresponding to the spectra in part A. All systems include 5 mL of HEPES solution (0.04 M), 0.1 mL of NaOH (1 M), and $HAuCl_4$ solutions (24.28 mM) from 40 to 115 μL. Spectra were recorded after the mixture reacted for 20 min. The bar is 50 nm.

All Raman spectra were recorded using a Renishaw Invia microscope Raman spectrometer. The spectrometer consists of a Leica confocal microscope, a grating of 1200 mm^{-1} and a Peltier cooled CCD detector. Raman measurements were performed with an excitation line provided by a He−Ne laser (633 or 785 nm wavelength) via a 50× long working distance objective lens, of which the NA is 0.50. The laser powers focused on samples are 1.2 mW for 785 nm and 0.176 mW for 633 nm when the attenuation by the air between the samples and the objective lens is not taken into account. It should be noted that the exposure times (10 s) are the same for all the Raman spectra.

RESULTS AND DISCUSSION

Controllable Synthesis of Gold Nanostars. The nanostars with tunable LSPR were prepared under the previous literature.[15] In the previous literature, the authors developed a protocol using HEPES to synthesis gold nanostars. They mentioned that an increase in the $HAuCl_4$ concentration led to the proliferation of irregularly shaped and spherical gold nanoparticles in the products. Base on the above information, we quantize the relationship between the $HAuCl_4$ concentration and the optical properties of the products. The extinction spectra of the products are shown in Figure 1A for a fixed time interval of 20 min. This time interval was selected since extinction peak of gold nanostars reached an almost saturation value after this period (see Figure 1s in the Supporting Information). As shown in Figure 1Aa, the extinction spectrum shows two LSPR peaks (522 and 704 nm). According to the calculations by Hao et al.[18,19] and Kumar et al.,[12] these bands of branched particles are attributed to dipole resonances, localized at either the tips or the central core of the particles. The

Scheme 1. Fabrication of SERS Active Substrate with Gold Nanostars Using Electrostatically Assisted APTES-Functionalized Surface-Assembly Method

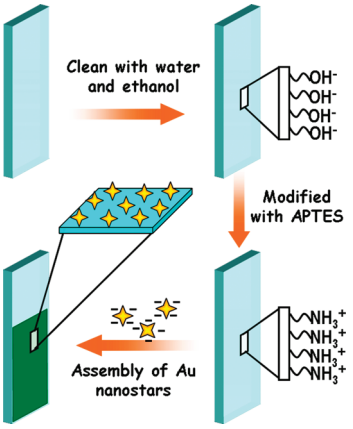

locations of these bands are sensitive to the length and sharpness of the branch.[18] Therefore, heterogeneity in the number of the branches should only have a minor effect on the spectrum. The peak at 704 nm is mainly caused by the longitudinal plasmon resonance which is proportional to the length of branches; and the other peak at ca. 522 nm could mainly caused by the dipole resonance, located at the branching points. Furthermore, when it comes to the experimental extinction spectrum, plasmon hybridization should be taken into account. The longitudinal plasmon resonance of gold nanostars could be controlled by varying the concentration of $HAuCl_4$. As the concentration of $HAuCl_4$ decreases, the longitudinal plasmon resonance peak red-shifts, this can be attributed to the structurally increased branch-length and TEM images in part B confirm this. In Figure 1B, the nanostar branch-length decreases obviously from (a) to (d) with the increasing of $HAuCl_4$ concentration. Specially, the extinction spectrum shows only one SPR peak (Figure 1A, spectrum d) when the concentration of $HAuCl_4$ solution is higher than 550 μM, indicating the formation of gold nanospheres with bulges instead of gold nanostars (Figure 1B, d). The calibration curve corresponding to the longitudinal plasmon resonance wavelength of the resulting gold nanostars at different concentrations of $HAuCl_4$ is presented as the insert in Figure 1A. As it shows, the wavelength decreases linearly with $HAuCl_4$ concentration, implying that the resonant wavelengths of gold nanostars are tunable.

Assembly of SERS Substrates. electrostatically assisted APTES-functionalized surface-assembly method (Scheme 1) was chosen for the fabrication of SERS substrates. The most attractive advantage of electrostatically assisted APTES-functionalized surface-assembly method is that a substrate with a very homogeneous SERS signal and large area (up to several square centimeters) can be fabricated in a normal laboratory without complicated equipment. This is preponderant in commercial manufacture. In order to form a uniform substrate, capping agents are usually requisite to prevent the aggregation of nanoparticles during the synthesis process. Stirring was involved during the star-assembly step in order to further increasing the homogeneousness of the obtained substrates. Samples a−d (ordered in Figure 1B) were all assembled on the ITO surfaces, which were called substrates a−d, respectively, in the following discussion, for studying the influence of the SERS efficiency across nanostar morphology.

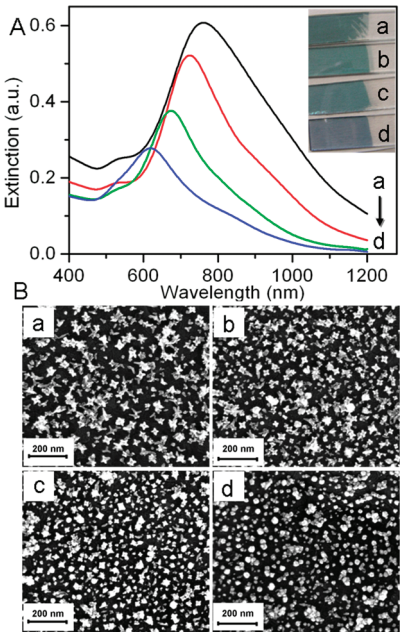

Figure 2. (A) UV−vis−NIR spectra, (A inset) photographs, and (B) SEM images of substrates a−d assembled with nanostar samples a−d. The bar is 200 nm.

The corresponding extinction spectra and digital photographs of substrates a to d were ordered in Figure 2A and SEM images of substrates a−d were also ordered in Figure 2B. Compared with the spectra of the solutions, the spectra obtained on ITO surfaces were somewhat broader. Moreover, the longitudinal SPR peaks of the substrates all red shift about 50 nm. The reason might be the changes of interparticle distance when adsorbed on ITO surfaces: the gold nanostars are aggregated when adsorbed on ITO surfaces (Figure 2B). The aggregation is possibly ascribed to the high concentration of gold nanostars in solution before self-assembly and the polarization of gold nanostars aroused by the positive charged amino group of APTES.[16,26,27]

To clearly demonstrate the advantages of the APTES-functionalized fabrication technique, we also made SERS substrates using the same fabrication process with blank ITO glass slips. Their SERS signal strengths and uniformity were compared with the APTES-functionalized ones. As shown in Figure 3A, the SERS signal strength of functionalized substrate is about 10-fold higher than the blank substrate. Panels B and C in Figure 3 show the uniformity test performed on the functionalized and blank substrates. Nine random points, separated by millimeter distances, were measured. Briefly, the SERS spectra are characterized by ring stretching (1492, 1440, 1387, 1351, and 1325 cm^{-1}), CH bending (1202, 1185 cm^{-1}), and the in-plane CCC and NCC (673 cm^{-1}), CCC and CNC (595 cm^{-1}), and CCC (499 cm^{-1}) deformations.[20] In Figure 3B, as can be observed, extremely good reproducibility is achieved in the characteristic peaks of NBA at 499, 595, 673, 1185, and 1440 cm^{-1}. The peak height at 595 cm^{-1} was treated statistically for each spectrum. The results show a mean value of the peak height of 33389 $\pm$ 651 counts, which is equivalent to a 2% standard deviation. In part C, the standard deviation of peak height at 595 cm^{-1} is 54%, which is much worse than the functionalized substrate. In conclusion, our fabrication step using APTES functionalization greatly improves the uniformity as well as the SERS intensity of the fabricated substrates.

Influence of Nanostar Morphology. In this part, the SERS efficiency of four substrates prepared above were investigated and compared in order to study the morphological influence of nanostar (branch-length). For the SERS measurement here, the laser spot covers arrange of several micrometers containing several hundred nanostars and the resulting signal is a summation of the signals from analytes that absorbed on these nanostars, so a fair comparison between substrates a to d is achievable only if the number of sampled analyte molecules adsorbed on substrates is kept constant between the particle shapes. NBA with positive charge was used as the sampled analyte in the following SERS measurements. The nanostars are synthesized with a coating of HEPES, which presents negative charges, bringing the positive charged NBA within close proximity of the enhanced E-fields. Thus, the number of analytes is determined by the total gold surface areas on the substrate covered by the laser spot.

To estimate total gold surface areas on each subatrate, we proposed a 3D nanostar model referred to by Khoury et al.[21] in Figure 2s in the Supporting Information, where a nanostar is interpreted as a spherical core of diameter D, from which originates a number, N, of round-end cone "branches". The core is measured as the central sphere on top of which protrusions are formed. A branch is defined as any well-formed protrusion that is longer than 2 nm for modeling purposes. Otherwise, the protrusion is defined as surface roughness only. The branch is governed by the parameters of branch base D_a, branch length L, and branch tip D_b. The model's dimensions for samples a to d are estimated in Table 1. These were calculated by analyzing hundreds of particles in more than one TEM and SEM images. Table 1s in the Supporting Information enabled the estimation of average gold surface areas of 2.39, 2.09, 1.87, and 1.52×10^3 nm^2 for a generic nanostar in samples a to d, respectively. Furthermore, the total numbers of nanostars in 1×10^6 nm^2 calculated in SEM images are 323, 369, 416, and 521 in substrates a to d, respectively. So the total gold surface areas of substrates a to d under the 20.0 μm $\times$ 5.0 μm laser spot are about 7.72, 7.71, 7.78, and 7.92×10^7 nm^2 respectively. Distinctly, the total gold surface areas of four substrates are almost equal.

It is also noteworthy that the decreasing overlap of the leading edge of the longitudinal plasmon band and the 785 nm excitation source, as star branch length decreases, would hypothetically also be accompanied by an observable decrease in intensity. In order to find out that whether it plays the major role in influencing SERS intensity, a 633 nm excitation source was also used, the overlap of the leading edge of which and the longitudinal plasmon band increases as star branch length decreases.

The SERS efficiencies of four substrates were investigated, and their spectra are displayed in Figure 4 (substrates a–d correspond to spectra a–d). The intensity at 595 cm^{-1} Raman band was selected as the comparative analysis signal. It is obvious that the substrate with the longest branch-length exhibits the most intense SERS signal, whether the excitation source is 785 or 633 nm. This is different from the results on nanostars in solution.[21] Considering that the four substrates have almost the same gold surface areas and other experiment conditions (such as excitation source and the laser power) were controlled to be the same as well, it could be concluded that the nanostar branch length here is the primary reason that effect the substrate' SERS intensity. Herein, substrate a is the most active substrate for SERS, especially under the 785 nm excitation source. As a result, substrate a was used for the following SERS measurements as the 785 nm excitation source was chosen for further studies.

SERS Measurements. On the basis of the above studies, substrate a was used for the following SERS measurements. In this part, two organic molecules, NBA and R6G, were used to testify the SERS activities of the substrates. The latter molecule, R6G, is often employed in SERS studies because of its large Raman cross-section, and was used herein in order to compare the enhancement of our substrate with others in earlier publications.[22−24]

Figure 5A shows the obtained SERS spectra when NBA solutions with different concentrations (5×10^{-11} M up to 5×10^{-9} M) were tested. Five $\times 10^{-12}$ M NBA did not show any characteristic peaks, and thus the 5×10^{-11} M concentration is taken as the limit of detection for the NBA molecule. Spectra d in

Table 1. Average Nanostar Dimensions Estimated by Measuring 100 Particles Imaged under TEM and SEM[a]

star sample	D (nm)	L (nm)	D_a (nm)	D_b (nm)	N
a	21 ± 2	20 ± 3	12 ± 1	6 ± 1	4 ± 2
b	22 ± 2	13 ± 2	13 ± 1		
c	22 ± 2	7 ± 2	12 ± 1		
d	22 ± 2				

[a] Samples a–d correspond to images a–d in Figure 1B.

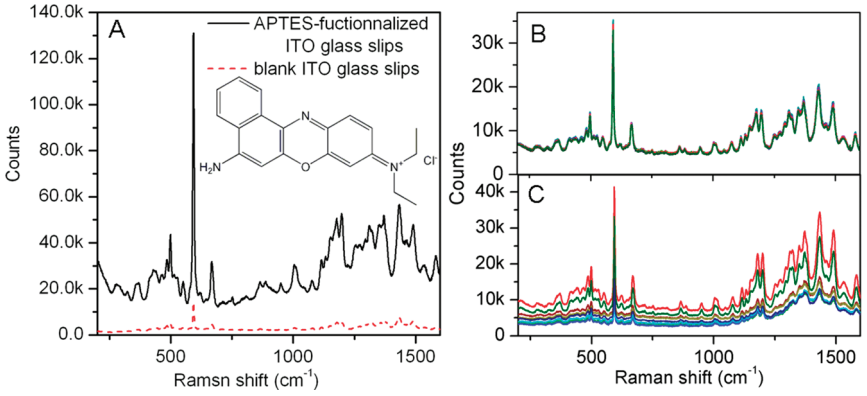

Figure 3. (A) Comparison of SERS signal strengths with the blank substrate and APTES-functionalize substrate. Both substrates were immersed in a NBA solution with the concentration of 1×10^{-7} M. (B, C) Raw data for uniformity tests of the (B) functionalized substrate and (C) blank substrate. Nine random points, separated by millimeter distances, were measured. All SERS spectra were measured under the 785 nm excitation source. The laser power is focused on samples is 1.2 mW. The exposure time was 10 s. The NBA structure is shown as the inset in part A.

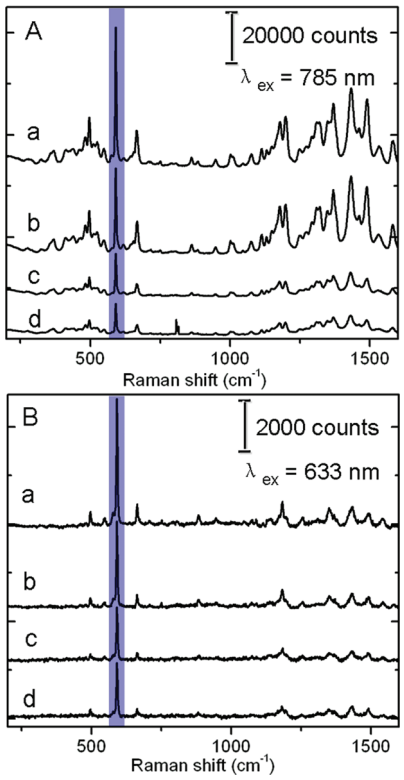

Figure 4. SERS spectra of NBA at a concentration of 5×10^{-8} M for substrates a to d under different laser wavelength: (A) 785 nm and (B) 633 nm. Laser power of 785 and 633 nm is 1.2 and 0.176 mW, respectively. Seven random points, separated by millimeter distances in one substrate, were measured. Each SERS spectrum was the result of averaging those 7 scans. The exposure time was 10 s.

Figure 5A is the Raman spectra of a 2×10^{-3} M NBA solution obtained when using the ITO glass acting as a non-SERS substrate. This high concentration was necessary in order to be able to directly compare the SERS-active substrate with a non-SERS substrate because the ITO glass surface did not show any Raman signal when the NBA concentration was lower than 2×10^{-3} M. By direct comparison of spectra a and d, it is possible to demonstrate the large enhancement due to the gold nanostar substrate.

Because the surface enhancement factor (EF) is found to have many definitions in other literatures.[25,11] In this paper, it is calculated by using the analytical chemistry point of view through the analytical EF (AEF) defined as[25]

$$\mathrm{AEF} = (I_{\mathrm{SERS}}/C_{\mathrm{SERS}})/(I_{\mathrm{RS}}/C_{\mathrm{RS}})$$

where I_{SERS} corresponds to the Raman intensity obtained for the SERS substrate under a certain concentration C_{SERS} and I_{RS} corresponds to the Raman intensity obtained under non-SERS conditions at an analyte concentration of C_{RS}. The experimental conditions, such as the laser wavelength, laser power, microscope objective or lenses, spectrometer, and measuring conditions on the substrate, are taken into account and are identical in all cases.

According to this established definition, the AEF of the substrate was estimated by considering the 595 cm^{-1} Raman band, because it is the strongest peak of all bands in the spectra. When using $C_{\mathrm{SERS}} = 5 \times 10^{-10}$ M and $C_{\mathrm{RS}} = 2 \times 10^{-3}$ M and the intensities obtained from Figure 5A, we can obtain a value of

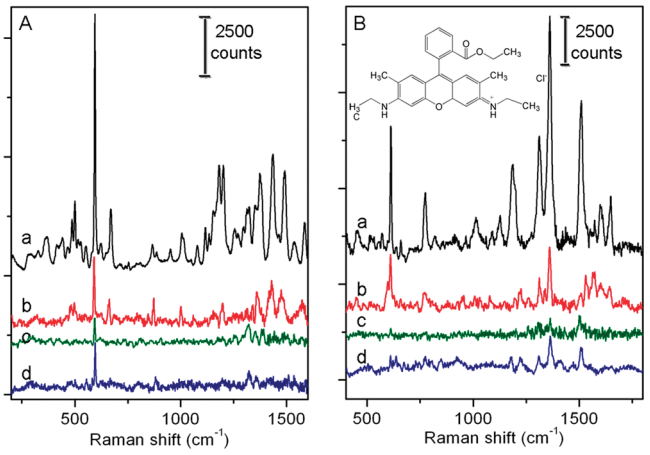

Figure 5. Raman spectra obtained using the NBA and R6G molecule. (A) Spectra measured while substrate a was immersed in a solution with NBA concentrations of (a) 5×10^{-9} M, (b) 5×10^{-10} M, and (c) 5×10^{-11} M; (d) the spectrum measured while a non-SERS substrate was immersed in a solution with NBA concentration of 2×10^{-3} M. (B) Spectra measured while substrate a was immersed in a solution with R6G concentrations of (a) 1×10^{-7} M, (b) 1×10^{-8} M, and (c) 1×10^{-9} M; the spectrum measured while a non-SERS substrate was immersed in a solution with R6G concentration of (d) 1×10^{-3} M. The R6G structure is shown as the inset in part B. Seven random points, separated by millimeter distances in one substrate, were measured. Each SERS spectrum was the result of averaging those 7 scans. The wavelength of the excitation source is 785 nm and the exposure time was 10 s.

AEF = 5×10^6. It should be noted that the AEF is different when different Raman band or C_{SERS} are chosen for estimation. But those AEFs are the same order of magnitude (see Table 1S in the Supporting Information). Furthermore, the AEF increases with the increases of branch length generally (see Table 2S in the Supporting Information).

Figure 5B shows the spectra obtained when the substrate a was immersed in R6G solutions of different concentrations, following the same procedure from low to high concentration as that in the NBA measurements. In this case, a concentration of 1×10^{-9} M was able to be detected, as shown in spectrum c of Figure 5B. This detection limit is 10-fold higher than the self-assembled monolayer of silver nanocrystals superlattice reported by Qiu et al.[22] Compared to their hydrothermal method, our fabricating strategy is at room temperature and more convenient. Further comparisons show that the detection limit of our substrate is equal to the Au-coated ZnO nanorod array on Si (100) substrate made by Sakano et al.[23] and lower than the gold flowerlike nanoarchitectures on indium tin oxide coated glass substrate made by Duan et al.[24] More details for their SERS measurement conditions are provided as Supporting Information.

Spectra d in Figure 5B is the Raman spectra of a 1×10^{-3} M R6G solution obtained when using the ITO glass acting as a non-SERS substrate. It is clearly shown that the signal intensity for the 1362 cm^{-1} peak is extremely weak when compared to the ones using the nanostar substrate with much lower concentrations. When using this concentration as C_{RS} and a concentration of 1×10^{-8} M as C_{SERS} and using the obtained intensities shown in Figure 5B, it is possible to establish a value of AEF = 2×10^5 when using R6G as the analyte. Compared to the AEF value obtained on NBA, the AEF of R6G is smaller. It can be pointed out that the amount of molecules present on the R6G SERS is smaller because of the different molecular size. Additionally,

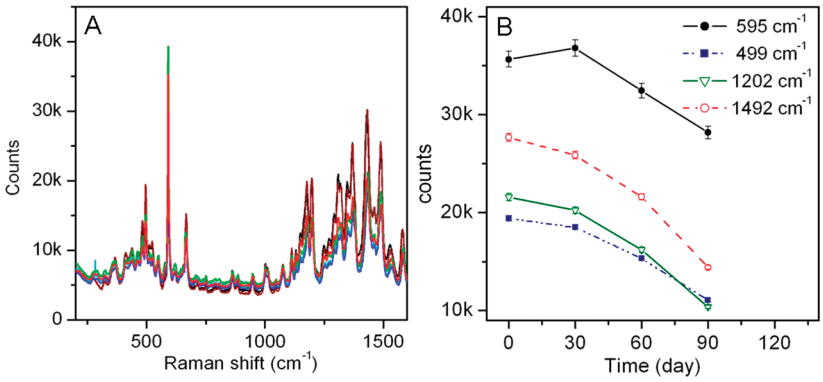

Figure 6. (A) Raw data for the substrate reproducibility tests. The SERS spectra of six substrates were measured. (B) Stability of SERS activity of the as-fabricated substrates.

there may be difference in the chemical enhancement between the two molecules. However, as the interactions between the two analytes and the nanostar substrates are very similar, we believe that this decrease in the number of molecules can be the main reason for the lower SERS signal observed with R6G.

In addition to the uniformity of the substrate tested in Figure 3B, the reproducibility between substrates was also tested. Six substrates, made at different time, were measured and shown in Figure 6A. The deviation of peak height at 595 cm^{-1} is 7.3%. The reproducibility of these data is worse than that in Figure 3B. Besides the good reproducibility, our substrates display quite stable SERS enhancements (Figure 6C). After 90 days (store at 4 °C), the SERS enhancements are reduced by only 50% relative to measurements performed on freshly prepared array substrates.

CONCLUSIONS

In conclusion, a low-cost SERS active substrate with very good reproducibility has been prepared by electrostatically assisted APTES-functionalized surface-assembly of gold nanostars with controllable morphology. The SERS efficiency of substrates assembled by gold nanostars with different branch-lengths were investigated and compared. It found that substrate assembled by the nanostars with the longest branches generated the biggest enhancement when other experimental conditions (such as the laser frequency and power) were controlled to be the same. Simplicity in the production of the gold nanostar films compared to expensive lithographic methodologies combined with the excellent reproducibility and high Raman EFs provide an exceptionally cost-effective substrate for SERS analysis. Two different target molecules were examined to determine the SERS activity of the presented substrate. A concentration of 5×10^{-11} M was detectable for NBA, and R6G with a concentration of 1×10^{-9} M was clearly detected. Final AEFs can be estimated as 5×10^{6} for NBA and 2×10^{5} for R6G.

ASSOCIATED CONTENT

Supporting Information. The longitudinal plasmon resonance wavelength versus time curve corresponding to the resulting gold nanostars, nanostar model schematic, average nanostar dimensions estimated by measuring 100 particles imaged under TEM and SEM (PDF). This material is available free of charge via the Internet at http://pubs.acs.org.

AUTHOR INFORMATION

Corresponding Author

*Tel/fax: +862583795719. E-mail: wqian@seu.edu.cn.

ACKNOWLEDGMENT

We gratefully acknowledge the support from National Natural Science Foundation of China (Grant 90923010), Chinese 973 project (Grant 2010CB933902), and Specialized Research Fund for the Doctoral Program of Higher Education of China (Grant 20090092110026).

REFERENCES

(1) Bell, S. E. J.; Sirimuthu, N. M. S. *J. Am. Chem. Soc.* **2006**, *128* 15580–15581.
(2) Kneipp, K.; Kneipp, H.; Itzkan, I.; Dasari, R. R.; Feld, M. S. *Chem. Rev.* **1999**, *99*, 2957–2975.
(3) Nie, S. M.; Emory, S. R. *Science* **1997**, *275*, 1102–1106.
(4) Sackmann, M.; Materny, A. *J. Raman Spectrosc.* **2006**, *37*, 305–310.
(5) Campion, A.; Kambhampati, P. *Chem. Soc. Rev.* **1998**, *27*, 241–250.
(6) Esenturk, E. N.; Walker, A. R. H. *J. Raman Spectrosc.* **2009**, *40* 86–91.
(7) Lin, X. M.; Cui, Y.; Xu, Y. H.; Ren, B.; Tian, Z. Q. *Anal. Bioanal. Chem.* **2009**, *394*, 1729–1745.
(8) Murray, R. W. *Chem. Rev.* **2008**, *108*, 2688–2720.
(9) Liz-Marzán, L. M. *Langmuir* **2006**, *22*, 32–41.
(10) Grzelczak, M.; Pérez-Juste, J.; Mulvaney, P.; Liz-Marzán, L. M. *Chem. Soc. Rev.* **2008**, *37*, 1783–1791.
(11) Natan, M. J. *Faraday Discuss.* **2006**, *132*, 321–328.
(12) Kumar, P. S.; Pastoriza-Santos, I.; Rodríguez-González, B.; de Abajo, F. J. G.; Liz-Marzán, L. M. *Nanotechnology* **2008**, *19* 015606–015611.
(13) Rodríguez-Lorenzo, L.; Álvarez-Puebla, R. A.; Pastoriza-Santos, I.; Mazzucco, S.; Stéphan, O.; Kociak, M.; Liz-Marzán, L. M.; de Abajo, F. J. G. *J. Am. Chem. Soc.* **2009**, *131*, 4616–4618.
(14) Hrelescu, C.; Sau, T. K.; Rogach, A. L.; Jäckel, F.; Feldmann, J. *Appl. Phys. Lett.* **2009**, *94*, 153113.
(15) Xie, J. P.; Lee, J. Y.; Wang, D. I. C. *Chem. Mater.* **2007**, *19* 2823–2830.
(16) Wang, Y.; Qian, W. P.; Tan, Y.; Ding, S. H. *Biosens. Bioelectron.* **2008**, *23*, 1166–1170.
(17) Enders, D.; Nagao, T.; Pucci, A.; Nakayama, T. *Surf. Sci.* **2006**, *600*, L71–L75.
(18) Hao, E. C.; Bailey, R. C.; Schatz, G. C.; Hupp, J. T.; Li, S. Y. *Nano Lett.* **2004**, *4*, 327–330.
(19) Hao, F.; Nehl, C. L.; Hafner, J. H.; Nordlander, P. *Nano Lett.* **2007**, *7*, 729–732.

(20) Álvarez-Puebla, R. A.; Contreras-Cáceres, R.; Pastoriza-Santos, I.; Pérez-Juste, J.; Liz-Marzán, L. M. *Angew. Chem., Int. Ed.* **2009**, *48* 138–143.
(21) Khoury, C. G.; Vo-Dinh, T. *J. Phys. Chem. C* **2008**, *112* 18849–18859.
(22) Qiu, T.; Wu, X. L.; Shen, J. C.; Chu, P. K. *Appl. Phys. Lett.* **2006**, *89*, 131914.
(23) Sakano, T.; Tanaka, Y.; Nishimura, R.; Nedyalkov, N. N.; Atanasov, P. A.; Saiki, T.; Obara, M. *J. Phys. D: Appl. Phys.* **2008**, *41*, 235304.
(24) Duan, G. T.; Cai, W. P.; Luo, Y. Y.; Li, Z. G.; Li, Y. *Appl. Phys. Lett.* **2006**, *89*, 211905.
(25) Le Ru, E. C.; Blackie, E.; Meyer, M.; Etchegoin, P. G. *J. Phys. Chem. C* **2007**, *111*, 13794–13803.
(26) Tan, Y.; Ding, S. H.; Wang, Y.; Jing, A. H.; Qian, W. P. *J. Nanosci. Nanotechnol.* **2006**, *6*, 262–264.
(27) Grabar, K. C.; Smith, P. C.; Musick, M. D.; Davis, J. A.; Walter, D. G.; Jackson, M. A.; Guthrie, A. P.; Natan, M. J. *J. Am. Chem. Soc.* **1996**, *118*, 1148–1153.